Intercalation of Sodium Ions into Hollow Iron Oxide Nanoparticles

Bonil Koo,[†] Soma Chattopadhyay,[⊥] Tomohiro Shibata,[⊥] Vitali B. Prakapenka,[‖] Christopher S. Johnson,[‡] Tijana Rajh,[†] and Elena V. Shevchenko*[†]

[†]Center for Nanoscale Materials, [‡]Chemical Sciences and Engineering, Argonne National Laboratory

[‖]Center for Advanced Radiation Sources, University of Chicago

[⊥]CSRRI-IIT, MRCAT, Bldg 433B, Argonne National Laboratory and Physics Department, Illinois Institute of Technology

*Corresponding authors: (T): +1-630-252-7633; (F): +1-630-252-5739 E-mail: bkoo@anl.gov; eshevchenko@anl.gov.

Supporting Information

Synthesis of core/shell NPs and their transformation into a hollow morphology

5.8 nm core / 2.8 nm shell iron/iron oxide NPs were obtained by air-oxidation of iron NPs synthesized in the presence of carbon nanotubes.[1] After annealing process at 200 °C for 12 hours, the core/shell NPs were transformed into the hollow NPs with a slightly increased shell thickness (Figure S1).

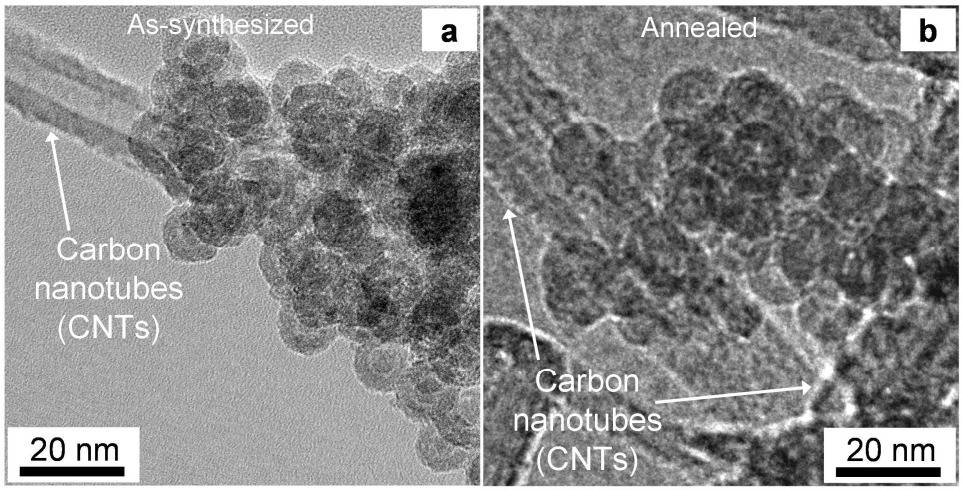

Figure S1. TEM images of (a) as-synthesized core/shell Fe/Fe_3O_4 NPs with carbon nanotubes and (b) hollow γ–Fe_2O_3 NPs obtained after annealing.

Synchrotron X-ray diffraction patterns and absorption spectroscopy on hollow NPs

XRD peaks of the hollow NPs are located at the same positions as those of bulk γ–Fe_2O_3 and XANES data obtained from the hollow NPs also showed similar near edge feature as standard γ–Fe_2O_3. However, the hollow NPs showed higher XRD peak intensity (~1.27 times) at (440) position, which corresponds with the presence of cation vacancies at octahedral sites.[1-3] Simulated XRD patterns confirmed that the inverse spinel γ–Fe_2O_3 structure with extra Fe vacancies at mainly octahedral sites shows higher (440) peak intensity. EXAFS study revealed the significantly low signal at Fe-Fe distance (2-3 Å) despite almost same intensity for Fe-O

signal (1-2 Å), which indicates that the first coordination shell (Fe-O6) structure of bulk γ–Fe_2O_3 and hollow NP is the same, but vacancies appear in the second neighbor Fe-Fe interactions. Also the edge features of hollow NP are similar as γ–Fe_2O_3 suggesting the oxidation states is the same.

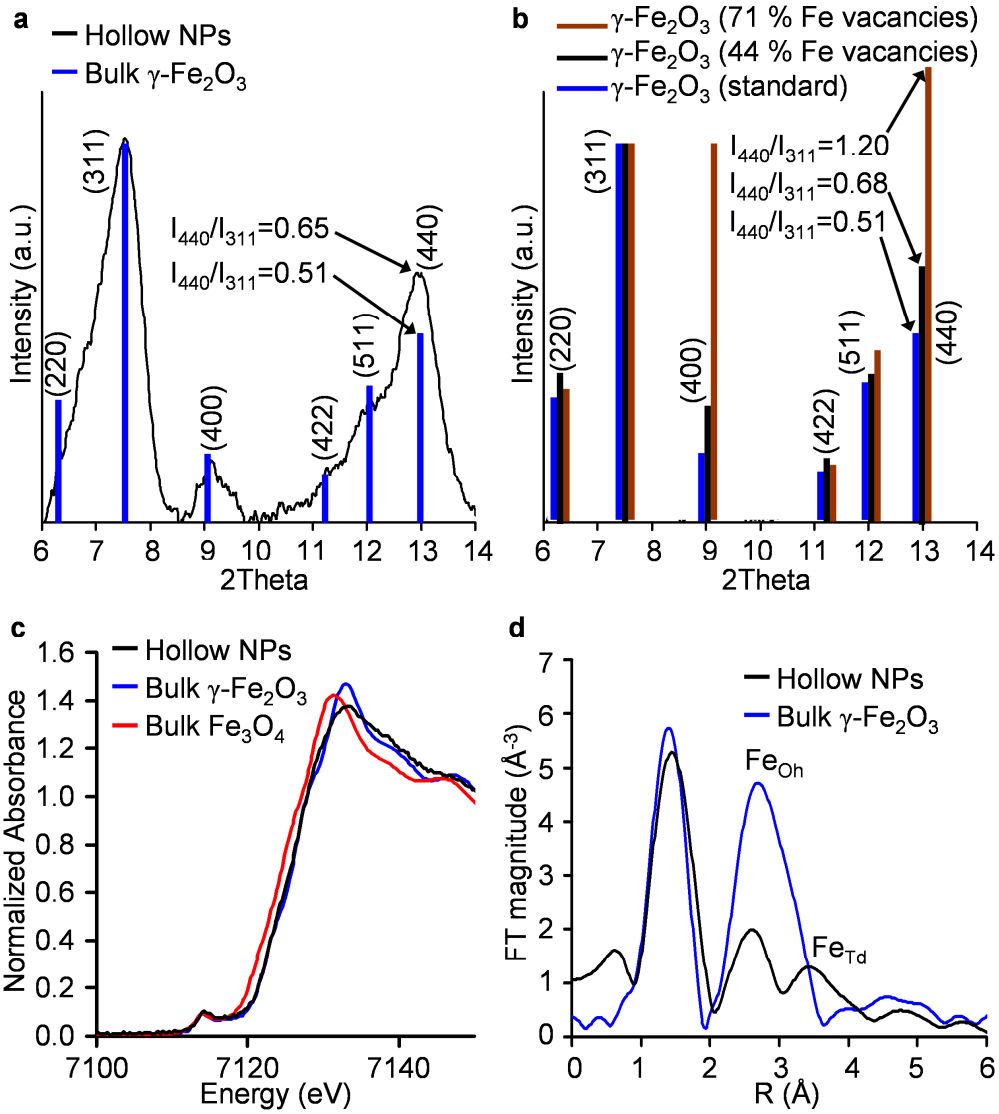

Figure S2. (a) XRD patterns of hollow γ–Fe_2O_3 NPs and (b) simulated XRD patterns with different concentration of Fe vacancies. (c) XANES and (d) EXAFS data measured on hollow γ–Fe_2O_3 NPs. The Fourier Transforms of k^2-weighted Fe EXAFS data were plotted in (d).

Na^+ ion conversion reaction of hollow iron oxide NPs with different electrode designs

Conventional battery electrode design (using carbon black and TAB binder) and layered composite design were compared in sodium ion conversion reaction of hollow NPs with working voltage of 3.0 - 0.01 V. Although layered composite electrode showed improvement of capacity retention, it still faded down after 10 cycles. TEM images of hollow NPs in layered composite before and after conversion reaction are shown in Figures S3b and S3c.

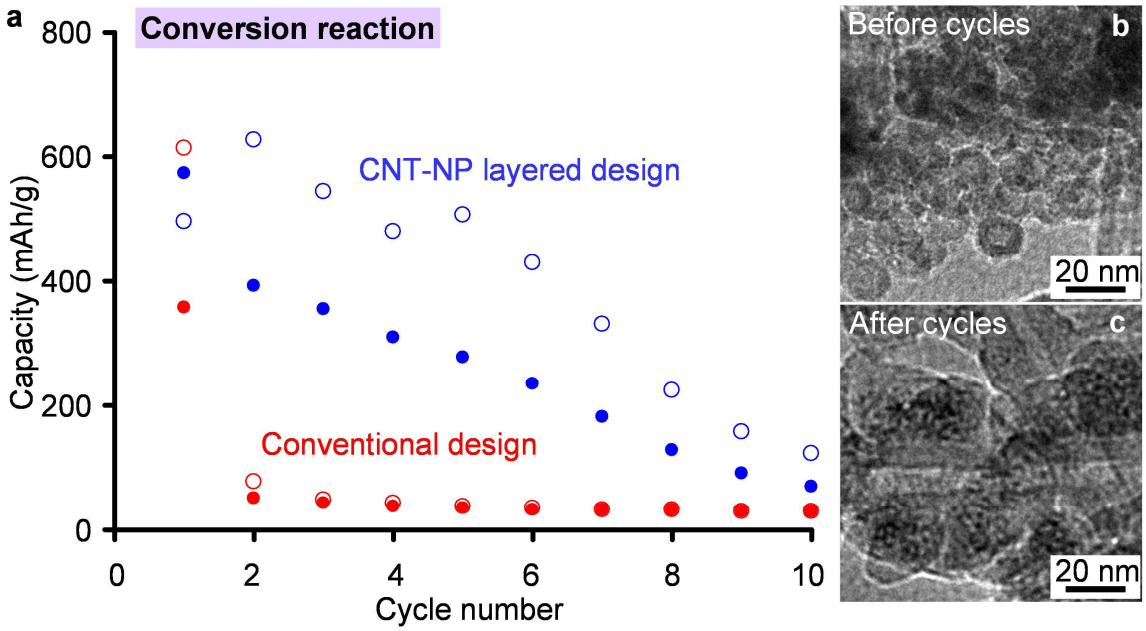

Figure S3. (a) Capacity versus cycle numbers of two different types of electrodes containing hollow γ–Fe_2O_3 NPs underwent Na^+ ion conversion reaction (3.0 – 0.01 V). TEM images of hollow NPs (b) before and (c) after conversion reaction cycles in layered composite electrode.

TEM images of hollow iron oxide NPs after Li^+ ion conversion reaction

Figure S4 showed that the morphology and the shape of hollow NPs in layered composite electrode were maintained after Li^+ ion conversion reaction.

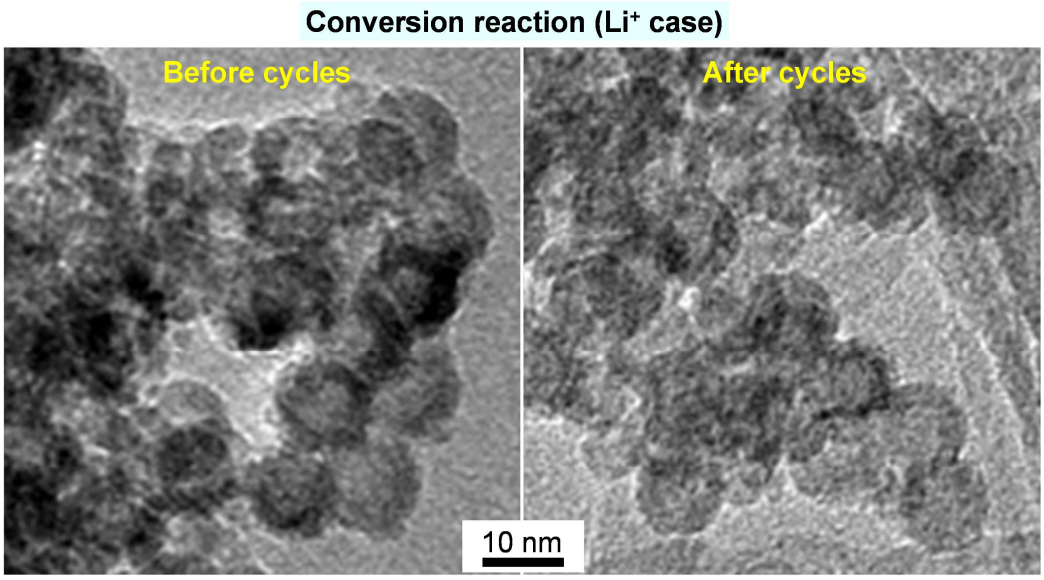

Figure S4. TEM images of hollow NPs before and after Li^+ ion conversion reaction (3.0 – 0.01 V).[1]

Na half cell test of pure CNT electrode

The pure CNT electrode was fabricated by the filtration of CNTs-IPA solution without the iron oxide NPs and tested with a Na metal counter electrode. The voltage profile during the first discharge in Figure S5 showed a negligible Na^+ insertion capacity up to 1.1 V.

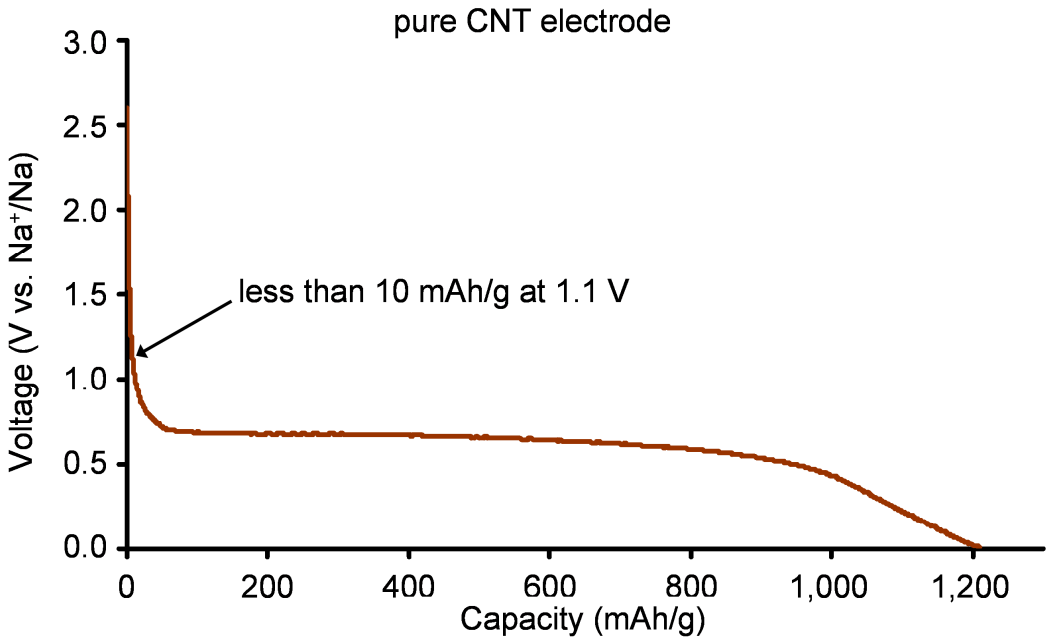

Figure S5. Voltage versus capacity profile of the pure CNT electrode.

Linear combination fitting (LCF) of XANES spectra

For each in situ XANES spectrum, the linear combination fits were obtained by operating a data processing software package Athena. XANES spectra of bulk γ–Fe_2O_3, bulk FeO, and Fe foil were used as the references for Fe(III), Fe(II), and Fe(0) respectively. The fits were plotted in the range of -20 ~ +20 eV from the edge energy (E_0 = ~7125 eV) after a relevant calibration and alignment of each fit. Each in situ XANES spectrum and its linear combination fit are shown with an indication of fit range in Figures S4 and S5, and the oxidation state numbers calculated from the fitting parameters (% of different oxidation state of Fe) are shown in Table S1.

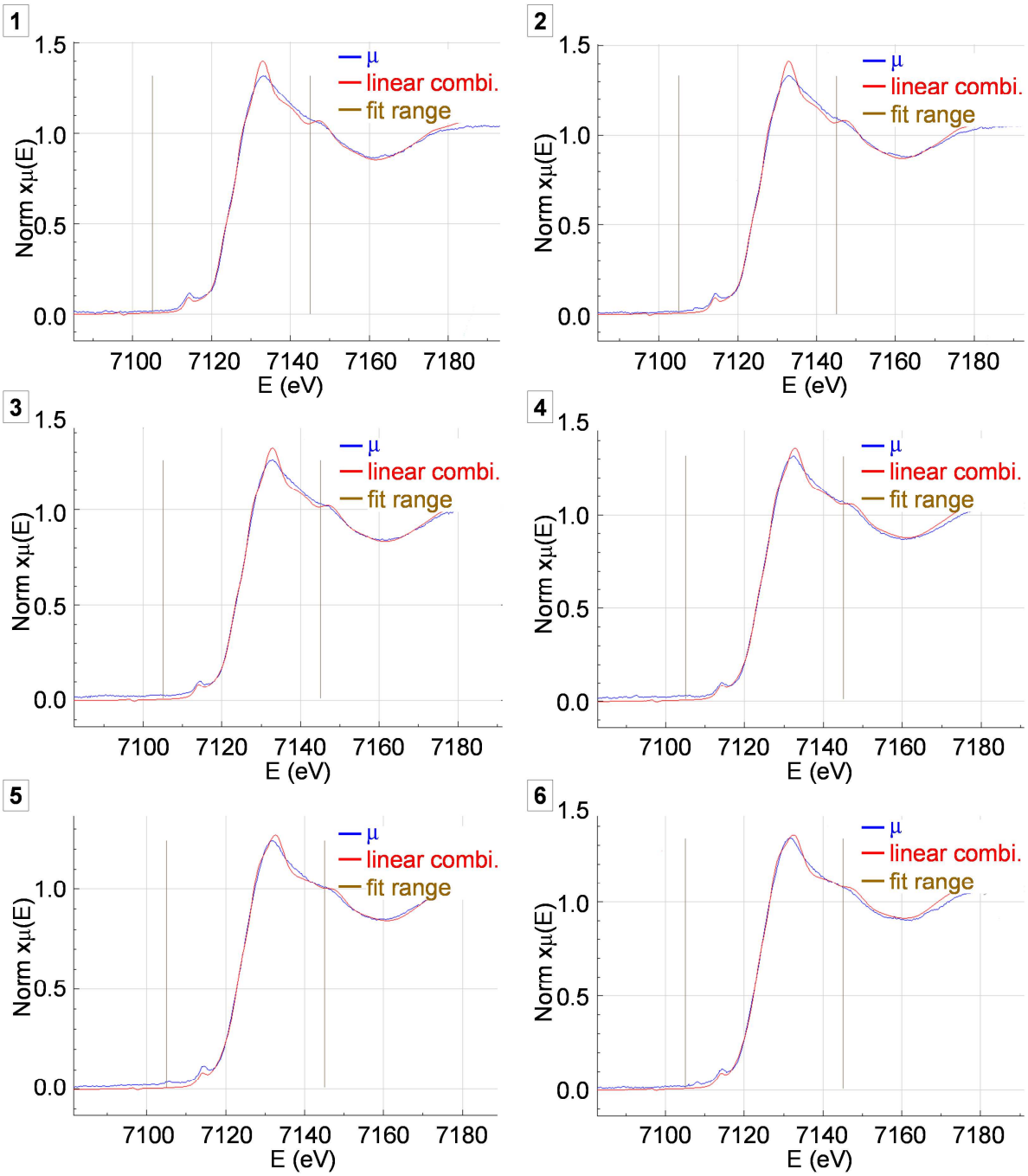

Figure S6. Plot of XANES spectrum of in situ sample (blue) and its linear combination fit (red) at data points 1 to 6. The fit range where the linear combination fitting was conducted is indicated as vertical lines.

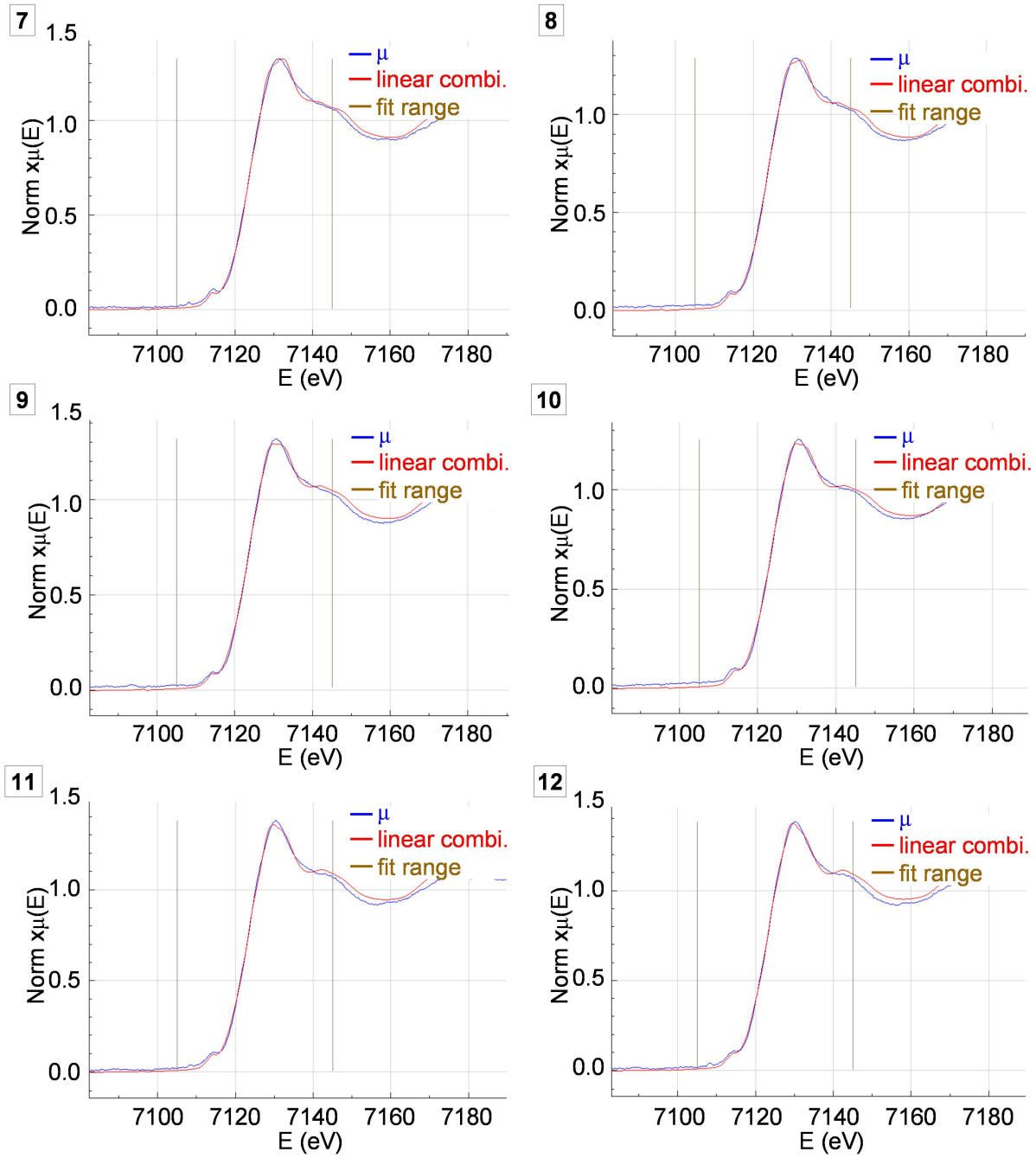

Figure S7. Plot of XANES spectrum of in situ sample (blue) and its linear combination fit (red) at data points 7 to 12. The fit range where the linear combination fitting was conducted is indicated as vertical lines.

Data point	1	2	3	4	5	6	7	8	9	10	11	12
Fe(II) (%)	8.9	11.8	17.4	24.6	32.2	36.2	42.1	45.3	50	49.8	54.6	57.7
Fe(III) (%)	91.1	88.2	82.6	75.4	67.8	63.8	57.9	54.7	50	46.2	43.4	39.8
Fe(0) (%)	0	0	0	0	0	0	0	0	0	4	2	2.5
Oxidation state	2.911	2.882	2.826	2.754	2.678	2.638	2.579	2.547	2.5	2.382	2.394	2.348

Table S1. The composition (%) of different oxidation state of Fe which the linear combination fitting used for each in situ data point and the oxidation state numbers calculated from the compositional analysis.

Coulombic efficiency *vs* cycle number

Plots of Coulombic efficiency *vs* cycle number for NP-CNT electrodes with different electrolyte salts were shown in Figure S8. Only the electrode with $NaClO_4$ tested at the slowest current rate showed an anomalous Coulombic efficiency at the initial cycles.

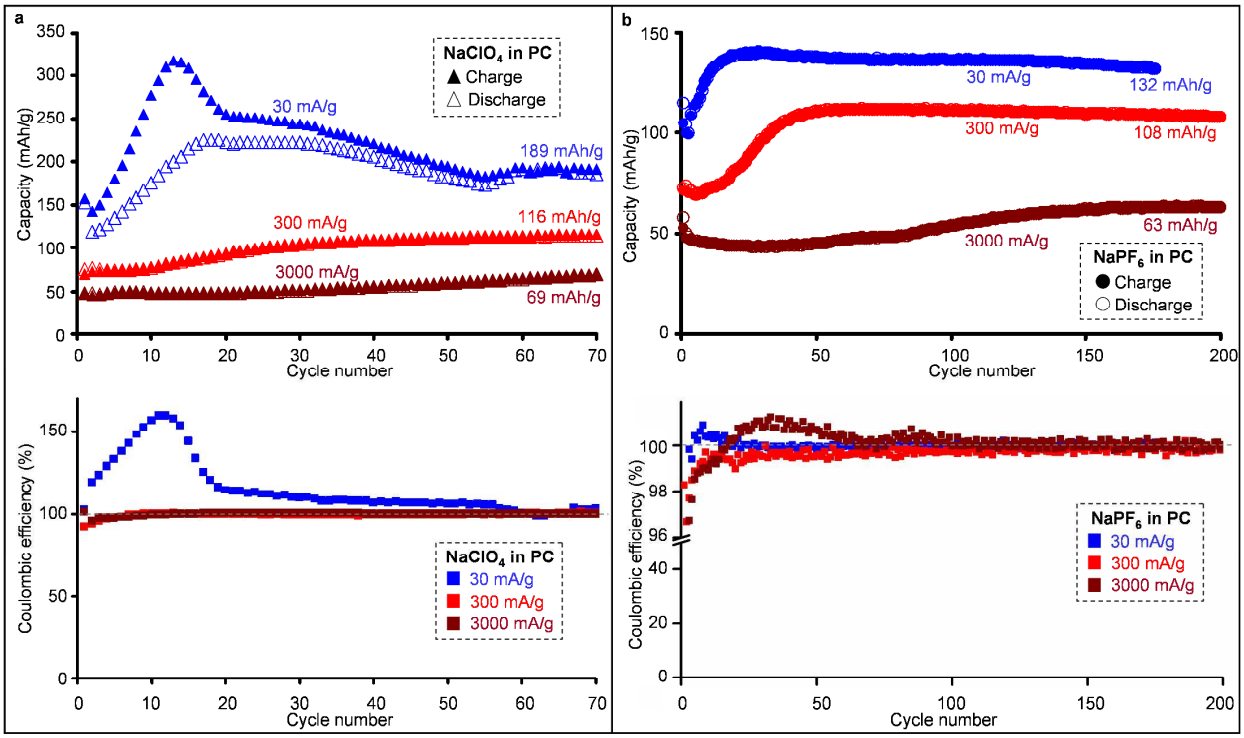

Figure S8. Coulombic efficiency versus cycle number of the NP-CNT electrodes with (a) $NaClO_4$ and (b) $NaPF_6$ electrolyte salts.

Capacity *vs* cycle number ($NaPF_6$ as electrolyte salt)

The NP-CNT electrodes that used $NaPF_6$ as an electrolyte salt showed a good capacity retention up to 500 cycles.

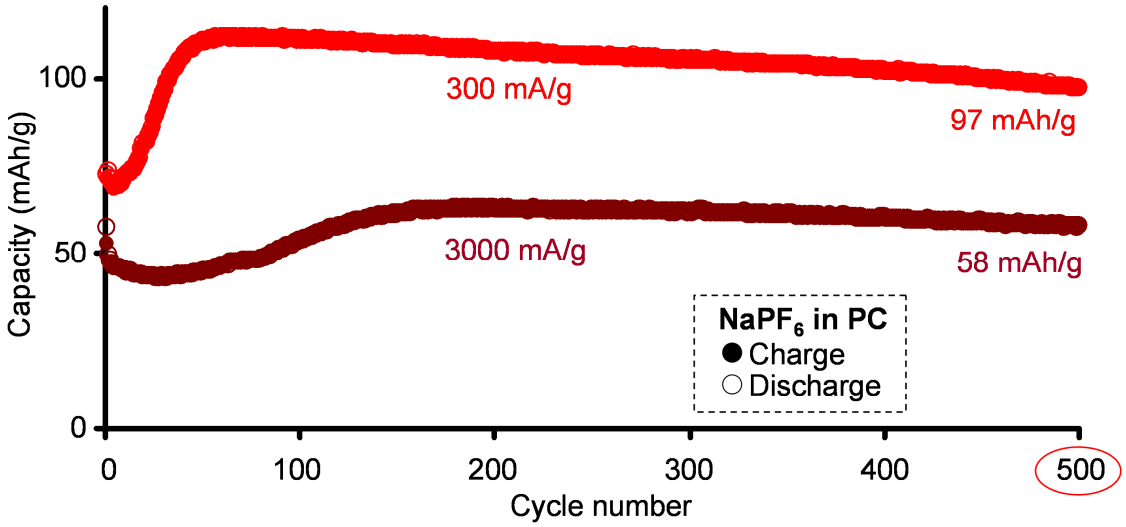

Figure S9. Capacity versus cycle number of the NP-CNT electrodes with $NaPF_6$ electrolyte salt.

REFERENCES.

(1) Koo, B.; Xiong, H.; Slater, M.; Prakapenka, V. B.; Balasubramanian, M.; Podsiadlo, P.; Johnson, C. S.; Rajh, T.; Shevchenko, E. V. *Nano Lett.* **2012**, *12*, 2429–2435.

(2) Greaves, C. *J. Solid State Chem.* **1983**, *49*, 325-333.

(3) Korobeinikova, A. V.; Fadeeva, V. I.; Reznitskii, L. A. *J. Struct. Chem.* **1976**, *17*, 737-741.